J. Phys. Chem. A **2003,** *107,* 6429−6440

Electronegativity, Resonance, and Steric Effects and the Structure of Monosubstituted Benzene Rings: An ab Initio MO Study

Anna Rita Campanelli

Department of Chemistry, University of Rome "La Sapienza", Città Universitaria, I-00185 Rome, Italy

Aldo Domenicano* and Fabio Ramondo

Department of Chemistry, Chemical Engineering and Materials, University of L'Aquila, I-67100 L'Aquila, Italy

Received: January 10, 2003; In Final Form: April 22, 2003

The deformation of the carbon skeleton of the benzene ring under substituent impact has been analyzed from the structures of 74 monosubstituted derivatives, as determined by ab initio MO calculations. The geometry of the substituted ring is shown to contain valuable information on the electronegativity, resonance, and steric effects of the substituent, and also on other, more subtle effects, affecting primarily the length of the $C_{ipso}-C_{ortho}$ bonds. The results obtained substantially augment previous knowledge from the analysis of experimental geometries (Domenicano, A.; Murray-Rust, P.; Vaciago, A. *Acta Crystallogr., Sect. B* **1983**, *39*, 457). Varying the electronegativity of the substituent causes a concerted change of the ring angles at the ipso, ortho, and para positions, coupled with a change in the $C_{ipso}-C_{ortho}$ bond length. The values of the ipso angle span a remarkably wide range, 113−126°. Enhancing the resonance interaction between a substituent and the ring causes a complex pattern of angular distortions, arising from the superposition of two separate effects. The first originates from the decreased length of the C−X bond, and consists primarily in a concerted change of the ipso and ortho angles. It occurs irrespective of whether the substituent is a π donor or a π acceptor. The second effect is associated with π-charge alternation on the ring carbons. It involves all the internal ring angles, and depends on the substituent being a π donor or a π acceptor. These angular changes are generally accompanied by changes in all C−C bond lengths, as expected from an enhanced contribution of polar canonical forms to the electronic structure of the molecule. By using symmetry coordinates, we have derived two orthogonal linear combinations of the internal ring angles, S_E and S_R, measuring the electronegativity and resonance effects of a substituent, respectively, as seen from their impact on the ring geometry. S_E and S_R values are affected in a typical way by steric effects.

1. Introduction

A prototypal organic molecule may be conceived as consisting of a hydrocarbon framework bonded to a substituent. The physical and chemical properties of the molecule, including its detailed structure, are determined by the valence electron distribution. It is expected that the geometry of the framework is perturbed by the presence of the substituent, and may reflect such effects as (i) the exchange of electron density between substituent and framework, (ii) the redistribution of electron density within the framework, and (iii) the steric interaction between substituent and framework.

The deformation of the regular hexagonal geometry of the benzene ring under substituent impact was first reported in 1956, in an electron diffraction study of the molecular structure of phenylsilane.[1] Reports from crystallographic[2] and spectroscopic[3] studies followed during the 1960s. Some important conclusions were drawn in the 1970s through the systematic analysis of many experimental geometries.[4−8] Substantial progress was made in 1983, through the statistical analysis of a large sample of monosubstituted benzene rings, the structures of which had been determined experimentally with reasonable accuracy.[9] Most of these structures were from X-ray crystallographic studies. It was found that the angular variance of monosubstituted benzene rings is described by two orthogonal components of distortion, involving angular changes in different ratios. The component accounting for most of the variance appears to be related to the σ-electronegativity of the substituent, the other to its π-donor/acceptor power. The separation of the two components was not based on chemical assumptions, but originated directly from the statistical analysis of the data. The interpretation of bond-length variation in chemical terms was less successful, however, since most of the bond-length variance was found to originate from systematic errors (such as uncorrected thermal motion effects) and other inhomogeneities of the sample. Using a different approach, attempts were also made to interpret the actual geometry of the substituted benzene ring in terms of a primary distortion (such as the change of the hybridization angles at the ring carbons from MO calculations), damped by the effect of geometrical constraints.[10−14] This hypothesis was found to be tenable for some substituents but not for others, notably those causing perturbations in the π-electron system of the benzene ring.

Molecular orbital (MO) calculations have been used repeatedly to study the deformation of the benzene ring caused by substitution.[10,13,15] The direct separation of the various components of geometrical distortion was never attempted, however. The present paper reports an analysis of the geometry of a large

---

* Corresponding author. Fax: 39-0862-433753. E-mail: domenica@univaq.it.

10.1021/jp030031r CCC: $25.00

sample of monosubstituted benzene rings from MO calculations. It is aimed at providing a detailed picture of the way in which the electronegativity, resonance, and steric effects of the substituent influence the skeletal geometry of the benzene ring. It is expected that the highly homogemeous nature of the data may disclose effects that were not revealed by the analysis of experimental data.

2. The Data Set

2.1. Origin of the Data. The structural data used in the present study refer to 74 monosubstituted benzene derivatives (plus unsubstituted benzene), the geometries of which have been determined by ab initio MO calculations at the HF/6-31G* level. This level was chosen because of its widespread use in the study of molecules of intermediate size. Its suitability to the scope of the present study was checked by HF/6-311++G** calculations, carried out on a large subset of the molecules investigated, and also by MP2(f.c.)/6-311++G** calculations. An effort has been made to construct a data set which is as much representative as possible of the different types of substituents, including extreme cases of inductive and resonance effects, sterically hindered species, and experimentally unaccessible conformations. Included are neutral molecules as well as anionic and cationic species. Substituents containing atoms heavier than chlorine have not been considered, as they are less amenable to HF/6-31G* calculations than substituents consisting entirely of light atoms. Only part of the entries of the data set are potential energy minima; many are saddle points on the potential energy hypersurface, as shown by harmonic normal-mode analysis.

We are aware, of course, that some of the optimized geometries in our data set may differ from true equilibrium geometries, due to inadequacies in the basis set used and neglect of electron correlation. This may especially apply to derivatives with negatively charged substituents. There is no doubt, however, that the various trends in structural variation emerging from the present study are all firmly established. Not only are they confirmed by the additional calculations mentioned above but also many of them have the support of experiment.[9] An analysis of the (minor) differences in structural variation resulting from the use of the 6-311++G** basis set at the HF, MP2, and DFT levels of theory is currently underway and will be the subject of a future paper.[16]

To identify the different conformations assumed by a nonlinear substituent, we make use of the following terms and abbreviations. *Coplanar conformation* (c): This term applies to planar substituents that are coplanar with the benzene ring, and also to substituents having C_{3v} symmetry when one of their symmetry planes coincides with the plane of the ring. *Orthogonal conformation* (o): This term applies to planar substituents when the substituent plane is orthogonal to the plane of the ring and passes through the ipso and para carbons. It also applies to substituents having C_{3v} symmetry when one of the symmetry planes of the substituent is orthogonal to the ring plane. *Pyramidal conformation* (p): We use this term specifically when the first atom of the substituent has a pyramidal bond configuration with a lone electron pair protruding from the ring plane, as in the equilibrium structure of aniline. *Equilibrium conformation* (e): We restrict the use of this term to the case of an equilibrium conformation that is neither coplanar nor orthogonal nor pyramidal.

All but three of the structures included in the data set have been optimized in our laboratory. The structure of biphenyl in its coplanar, orthogonal, and equilibrium conformations has been taken from the literature.[17]

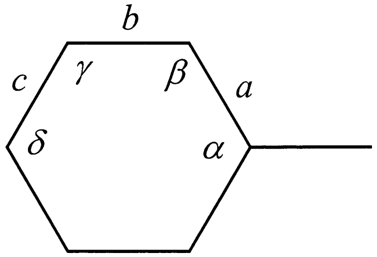

Figure 1. Lettering of the C−C bonds and C−C−C angles in a monosubstituted benzene ring of C_{2v} symmetry.

2.2. Treatment of the Data. The deformation of the carbon skeleton of the benzene ring caused by substitution usually conforms to C_{2v} symmetry (Figure 1). Small deviations from C_{2v} symmetry are known to occur with substituents lacking a 2-fold axis of symmetry.[18] This is the case of substituents having C_s symmetry (e.g., $CHCH_2$, CHO, OMe) or C_{3v} symmetry (e.g., BH_3^-, Me, SiF_3). When such substituents assume the coplanar conformation the $C_{ipso}\cdots C_{para}$ line is no longer a 2-fold axis of symmetry. The differences between corresponding C−C−C angles on opposite sides of the $C_{ipso}\cdots C_{para}$ line ($|\beta - \beta'|$ and $|\gamma - \gamma'|$) are generally small, only a few tenths of a degree; the largest values in the present data set occur with CHNH(c), 0.5°, OMe(c), 0.6°, and NHCOMe(c), 1.3°. The differences in length between corresponding C−C bonds on opposite sides of the $C_{ipso}\cdots C_{para}$ line ($|a - a'|$, $|b - b'|$, and $|c - c'|$) are also small, the largest values occurring with CMe_3(c) and PH_2(e), 0.007 Å, BPh_3^-(e), 0.009 Å, and OMe(c), 0.013 Å.

When a substituent having C_s or C_{3v} symmetry adopts the orthogonal conformation, then the primed and unprimed parameters remain equivalent, but the exact coplanarity of the ring atoms is lost. Deviations from planarity also occur when the ring symmetry is lowered to C_2 or C_1. In the present data set the deviations of the ring carbons from their least-squares plane are invariably small. The largest values, 0.005−0.006 Å, occur with BPh_3^-(e), $CONH_2$(e), SH(o), and SO_2Me(o).

Benzene ring deformations not conforming to C_{2v} symmetry span a much smaller range than those conforming to C_{2v} symmetry, at least as far as the carbon skeleton is concerned. Moreover, their actual extent depends—sometimes critically[19]—on the level of the MO calculations. For these reasons, and to simplify the analysis of the data, we have treated all benzene rings in our data set as having idealized C_{2v} symmetry, by averaging appropriate internal cooordinates and ignoring any out-of-plane deformation. A general distortion of a monosubstituted benzene ring can indeed be represented by three orthogonal components: (i) a distortion conforming to C_{2v} symmetry; (ii) a distortion from C_{2v} symmetry retaining the horizontal symmetry plane; (iii) a distortion from C_{2v} symmetry retaining the vertical symmetry plane. The present procedure discards the second and third components and reveals the first exactly.

The data set is presented in Table 1, giving also the molecular symmetry imposed in the optimization, the net π-charge transferred from the benzene ring to the substituent (or vice versa), and the structural substituent parameters S_E and S_R, as defined in section 5.6. π-Charges have been derived from the occupancies of the natural atomic orbitals of the ring carbons. For planar substituents, we have introduced the coplanar and orthogonal conformations as separate entries, as they always differ appreciably in energy and ring geometry. For substituents having C_{3v} symmetry, we have found, however, that the coplanar and orthogonal conformations are so close in energy and ring geometry that it would be inappropriate to treat them as separate

TABLE 1: C−C Bond Distances, Internal Ring Angles, Net Charge Transferred from the Substituent into the π System of the Benzene Ring, or Viceversa, and Structural Substituent Parameters S_E and S_R in Monosubstituted Benzene Derivatives, from ab Initio MO Calculations at the HF/6-31G* Level[a,b]

substituent[c]	molecular symmetry[d]	*a*	*b*	*c*	α	β	γ	δ	Δq_π[e]	S_E	S_R
H	D_{6h}	1.3862	1.3862	1.3862	120.00	120.00	120.00	120.00	0.00_0	0.00	0.28
Li	C_{2v}	1.4059	1.3879	1.3855	114.43	123.28	119.99	119.02	$+0.01_5$	−7.27	0.41
Be^+	C_{2v}	1.4082	1.3792	1.3895	119.02	120.31	119.69	120.98	$+0.06_9$	−0.80	1.31
BeH	C_{2v}	1.4015	1.3851	1.3860	116.61	121.97	119.81	119.82	$+0.01_6$	−4.32	0.82
BH_2(c)	C_{2v}	1.4004	1.3832	1.3874	117.66	121.40	119.56	120.41	$+0.09_9$	−2.93	1.33
BH_2(o)	C_{2v}	1.3945	1.3854	1.3852	117.94	121.10	120.19	119.48	-0.01_0	−2.61	−0.01
BH_3^-(o)	C_s	1.4018	1.3869	1.3870	114.97	122.89	120.43	118.39	-0.01_8	−6.63	−0.56
BPh_3^-(e)	S_4	1.4005	1.3874	1.3851	115.19	122.74	120.38	118.56	$+0.00_1$	−6.30	−0.43
BCl_2(c)	C_{2v}	1.4003	1.3824	1.3864	117.86	121.17	119.80	120.20	$+0.10_1$	−2.60	0.89
BCl_2(o)	C_{2v}	1.3933	1.3846	1.3854	118.60	120.73	120.06	119.82	$+0.01_4$	−1.72	0.27
CH_2^+(c)	C_{2v}	1.4365	1.3622	1.4030	119.12	120.16	118.87	122.81	$+0.55_1$	−0.25	3.33
CH_2^+(o)	C_{2v}	1.3933	1.3838	1.3859	122.10	118.28	120.44	120.47	$+0.00_5$	3.25	−0.28
CH_2^-(c)	C_{2v}	1.4482	1.3691	1.3993	113.13	122.54	122.86	116.07	-0.52_4	−7.96	−4.71
CH_2^-(o)	C_{2v}	1.4115	1.3879	1.3867	113.66	123.56	120.43	118.37	-0.01_8	−8.20	−0.41
Me(o)	C_s	1.3902	1.3855	1.3852	118.27	120.97	120.21	119.37	-0.00_9	−2.27	−0.13
CMe_3(c)	C_s	1.3937	1.3855	1.3839	117.16	121.54	120.40	118.96	-0.00_6	−3.68	−0.46
CMe_3(o)	C_s	1.3941	1.3856	1.3836	117.01	121.61	120.45	118.88	-0.00_6	−3.86	−0.55
$CHCH_2$(c)	C_s	1.3935	1.3837	1.3855	118.09	121.01	120.23	119.43	$+0.00_6$	−2.42	−0.10
$CHCH_2$(o)	C_s	1.3907	1.3856	1.3853	118.71	120.68	120.17	119.59	-0.00_3	−1.64	−0.01
Ph(c)	D_{2h}	1.3962	1.3838	1.3836	116.79	121.68	120.53	118.80	0.00_0	−4.10	−0.67
Ph(o)	D_{2d}	1.3907	1.3858	1.3854	118.72	120.67	120.17	119.59	0.00_0	−1.62	−0.01
Ph(e)[f]	D_2	1.3927	1.3847	1.3853	118.30	120.88	120.25	119.44	0.00_0	−2.15	−0.15
CCH	C_{2v}	1.3924	1.3835	1.3861	119.39	120.20	120.16	119.88	$+0.01_3$	−0.64	0.08
CHNH(c)	C_s	1.3907	1.3838	1.3865	119.32	120.36	119.98	120.00	$+0.03_5$	−0.83	0.38
CHNH(o)	C_s	1.3885	1.3853	1.3854	119.29	120.35	120.12	119.75	$+0.00_2$	−0.88	0.07
CN	C_{2v}	1.3905	1.3830	1.3865	120.48	119.58	120.02	120.33	$+0.03_1$	0.81	0.38
CHO(c)	C_s	1.3899	1.3834	1.3873	119.94	120.06	119.77	120.41	$+0.05_8$	−0.03	0.80
CHO(o)	C_s	1.3879	1.3851	1.3855	119.79	120.05	120.10	119.91	$+0.00_3$	−0.21	0.13
COCl(c)	C_s	1.3918	1.3826	1.3863	119.89	119.95	119.98	120.26	$+0.06_7$	0.02	0.46
COCl(o)	C_s	1.3862	1.3846	1.3856	120.64	119.52	120.11	120.10	$+0.00_7$	0.94	0.12
$CONH_2$(e)[g]	C_1	1.3901	1.3841	1.3860	119.45	120.27	119.99	120.03	$+0.03_7$	−0.64	0.37
COOH(c)	C_s	1.3901	1.3833	1.3865	120.03	119.92	119.91	120.31	$+0.05_4$	0.16	0.56
COOH(o)	C_s	1.3864	1.3849	1.3855	120.16	119.84	120.10	119.97	$+0.00_5$	0.26	0.12
COO^-(c)	C_{2v}	1.3900	1.3868	1.3869	118.36	120.99	120.12	119.43	$+0.00_8$	−2.22	0.01
COO^-(o)	C_{2v}	1.3918	1.3858	1.3865	117.73	121.25	120.42	118.92	-0.02_7	−3.00	−0.58
CF_3(o)	C_s	1.3864	1.3844	1.3856	120.27	119.79	120.04	120.08	$+0.02_0$	0.41	0.24
NH_2(c)	C_{2v}	1.3957	1.3825	1.3859	118.54	120.37	121.10	118.51	-0.13_0	−1.64	−1.76
NH_2(o)	C_{2v}	1.3903	1.3858	1.3855	118.65	120.75	120.11	119.63	-0.00_4	−1.74	0.10
NH_2(p)	C_s	1.3926	1.3835	1.3855	118.74	120.39	120.86	118.76	-0.09_7	−1.48	−1.34
NH_3^+(o)	C_s	1.3792	1.3851	1.3866	123.25	117.98	120.12	120.54	$+0.00_3$	4.34	0.04
NC	C_{2v}	1.3867	1.3836	1.3860	120.90	119.28	120.30	119.93	-0.00_8	1.32	−0.25
N_2^+	C_{2v}	1.3894	1.3789	1.3915	125.22	116.61	119.96	121.64	$+0.11_5$	7.27	0.61
NHCOMe(c)	C_s	1.3918	1.3840	1.3845	119.32	119.98	120.91	118.90	-0.06_5	−0.65	−1.40
NHCOMe(o)	C_s	1.3857	1.3851	1.3855	119.84	120.08	120.07	119.86	-0.00_1	−0.22	0.13
NO_2(c)	C_{2v}	1.3832	1.3833	1.3866	122.31	118.52	120.09	120.47	$+0.05_1$	3.15	0.15
NO_2(o)	C_{2v}	1.3781	1.3852	1.3859	122.89	118.21	120.18	120.33	-0.00_9	3.83	−0.11
O^-	C_{2v}	1.4393	1.3759	1.3943	113.63	122.53	122.16	116.99	-0.32_7	−7.44	−3.38
OH(c)	C_s	1.3869	1.3842	1.3857	120.20	119.60	120.72	119.16	-0.08_3	0.38	−1.12
OH(o)	C_s	1.3848	1.3855	1.3859	120.34	119.68	120.35	119.60	-0.03_6	0.48	−0.42
OMe(c)	C_s	1.3896	1.3845	1.3852	119.75	119.77	120.88	118.97	-0.08_4	−0.13	−1.37
OMe(o)	C_s	1.3856	1.3854	1.3860	120.30	119.69	120.36	119.59	-0.03_8	0.44	−0.44
OH_2^+(c)	C_{2v}	1.3692	1.3877	1.3865	126.37	116.09	120.43	120.59	-0.01_9	8.38	−0.69
OH_2^+(o)	C_{2v}	1.3725	1.3864	1.3879	126.19	116.25	120.14	121.03	$+0.00_5$	8.18	−0.06
F	C_{2v}	1.3783	1.3857	1.3863	122.34	118.47	120.50	119.71	-0.05_2	3.08	−0.79
Na	C_{2v}	1.4051	1.3889	1.3855	114.34	123.33	120.09	118.82	$+0.01_0$	−7.42	0.18
SiH_2^+(c)	C_{2v}	1.4155	1.3741	1.3931	119.17	120.21	119.43	121.55	$+0.21_2$	−0.49	1.93
SiH_2^+(o)	C_{2v}	1.4010	1.3814	1.3876	119.93	119.76	119.91	120.74	$+0.03_4$	0.33	0.80
SiH_2^-(c)	C_{2v}	1.4148	1.3787	1.3907	114.88	122.39	121.45	117.44	-0.25_2	−6.37	−2.37
SiH_2^-(o)	C_{2v}	1.4032	1.3886	1.3850	115.32	122.64	120.24	118.92	$+0.01_0$	−6.04	−0.07
SiH_3(o)	C_s	1.3956	1.3853	1.3855	117.86	121.21	119.94	119.84	$+0.01_5$	−2.70	0.52
$SiMe_3$(o)	C_s	1.3969	1.3857	1.3851	117.20	121.60	119.99	119.62	$+0.01_5$	−3.59	0.41
$SiPh_3$(e)	S_4	1.3975	1.3858	1.3852	117.38	121.46	120.02	119.67	$+0.02_0$	−3.31	0.38
SiF_3(o)	C_s	1.3958	1.3840	1.3860	118.69	120.70	119.83	120.25	$+0.01_8$	−1.55	0.78
PH_2(c)	C_{2v}	1.3927	1.3836	1.3852	119.05	120.22	120.71	119.08	-0.09_5	−1.04	−1.02
PH_2(o)	C_{2v}	1.3957	1.3849	1.3856	118.66	120.67	119.96	120.09	$+0.02_3$	−1.57	0.53
PH_2(p)	C_s	1.3914	1.3851	1.3851	118.57	120.73	120.22	119.52	-0.02_4	−1.80	−0.10
PH_2(e)[h]	C_s	1.3925	1.3855	1.3854	118.53	120.81	120.01	119.82	$+0.00_7$	−1.85	0.34
PH_3^+(o)	C_s	1.3957	1.3811	1.3881	121.02	119.18	119.88	120.87	$+0.04_4$	1.68	0.78
PPh_3^+(e)	S_4	1.3952	1.3835	1.3862	119.54	120.08	120.04	120.23	$+0.03_2$	−0.35	0.40
S^-	C_{2v}	1.4062	1.3836	1.3879	115.68	122.12	121.06	117.97	-0.15_3	−5.45	−1.67
SH(c)	C_s	1.3889	1.3846	1.3849	119.50	120.06	120.53	119.32	-0.06_4	−0.53	−0.71

TABLE 1: (Continued)

substituent[c]	molecular symmetry[d]	a	b	c	α	β	γ	δ	$\Delta q_{\pi}{}^{e}$	S_E	S_R
SH(o)	C_s	1.3887	1.3855	1.3854	119.66	120.11	120.11	119.90	-0.00_8	−0.36	0.12
$SO_2Me(o)^i$	C_s	1.3868	1.3845	1.3864	121.28	119.14	119.99	120.45	$+0.01_5$	1.82	0.38
Cl	C_{2v}	1.3830	1.3855	1.3854	121.28	119.07	120.40	119.77	-0.04_5	1.76	−0.51
$ClO_3(o)$	C_s	1.3784	1.3847	1.3866	124.26	117.33	120.16	120.77	$+0.00_4$	5.73	0.00

[a] Whenever necessary, the geometry of the monosubstituted benzene ring has been made consistent with C_{2v} symmetry by averaging appropriate geometrical parameters. [b] Bond distances are given in Å, angles and structural substituent parameters in deg, π-charges in electrons. [c] To identify the conformation of a nonlinear substituent with respect to the benzene ring we make use of the abbreviations (c), (o), (p), and (e). Of these, (c), (o), and (p) denote the coplanar, orthogonal, and pyramidal conformations, respectively, as defined in section 2.1, irrespective of whether they are minima or saddle points in the potential energy hypersurface. The abbreviation (e) denotes an equilibrium conformation that is neither coplanar nor orthogonal nor pyramidal. [d] Symmetry constraint imposed in the optimization of molecular geometry. [e] A positive sign indicates that electron density is transferred from the π system of the benzene ring into an appropriate orbital of the substituent; the opposite transfer is indicated by a negative sign. [f] In the minimum energy conformation of biphenyl, the two benzene rings are twisted by ca. 46°. [g] In the minimum energy conformation of benzamide, the $CONH_2$ group is twisted by ca. 22° about the exocyclic C−C bond. [h] In the minimum energy conformation of phenylphosphine, the plane of the PH_2 group is perpendicular to the ring plane, and makes an angle of 163.6° with the $C_{ipso}\cdots C_{ortho}$ line. [i] In this conformation of methylphenyl sulfone (corresponding to the potential energy minimum), the S-Me bond lies in a plane orthogonal to the ring plane, and one of the C−H bonds of the methyl group is syn to the S−Ph bond.

entries. So we have entered in the data set only the orthogonal conformation of these substituents. We made an exception for *tert*-butylbenzene, where the close proximity of the ortho hydrogens to some of the H atoms of the substituent makes the orthogonal conformation more sterically hindered than the coplanar.[20]

2.3. Calculations. MO calculations were carried out at the Hartree−Fock (HF) level with the 6-31G* basis set[21] and gradient optimization,[22] using the *Gaussian 98* package.[23] Apart from the symmetry constraints specified in Table 1, geometry optimization was otherwise complete. For 38 appropriately selected species (including nine with a negatively charged substituent) additional HF calculations were carried out with the 6-311++G** basis set. These were often followed by geometry optimization at the second order of the Møller−Plesset perturbation theory[24] (MP2, frozen-core approximation). Natural atomic and bond orbital analyses[25] were carried out using the *NBO 3.0* program.[26] Most calculations were run on an Alpha AXP-3000/500 cluster at the University of Rome "La Sapienza".

3. The Geometrical Parameters

3.1. Internal Coordinates. The carbon skeleton of a monosubstituted benzene ring of C_{2v} symmetry has, in general, three different bond distances (a, b, and c) and four different angles (α, β, γ, and δ), i.e., seven *internal coordinates* (Figure 1). These coordinates are not independent, due to two equations of geometrical constraint, expressing the conditions of planarity and ring closure. One of the equations is linear and imposes the constancy of the sum of the angles:

$$\alpha + 2\beta + 2\gamma + \delta = 4\pi \tag{1}$$

The other is nonlinear and involves bond distances as well as angles:

$$a \sin(\alpha/2) + b \sin(\beta + \alpha/2 - \pi) = c \sin(\delta/2) \tag{2}$$

In a statistical analysis of the internal coordinates the equations of geometrical constraint will introduce correlation. For instance $\alpha + \delta$ correlates exactly with $\beta + \gamma$, due to eq 1. If the constraint is nonlinear, the correlation will be nonlinear, but for small distortions of a benzene ring from D_{6h} symmetry, linear relationships give excellent approximations.[27]

To describe the deviation of the ring geometry from the reference geometry of unsubstituted benzene, where all angles are 120° and all C−C bonds have equal length, it is advantageous to use *internal distortion coordinates*, which we define as follows:

$$\Delta a = a - 1.3862 \text{ Å, etc.} \tag{3}$$

$$\Delta\alpha = \alpha - 120°\text{, etc.} \tag{4}$$

Here 1.3862 Å is the length of the C−C bond in benzene from both HF/6-31G* and HF/6-311++G** calculations.

3.2. Symmetry Coordinates. To describe the skeletal geometry of a monosubstituted benzene ring of C_{2v} symmetry we might arbitrarily select five internal coordinates, e.g., a, b, α, γ, and δ. It may not be obvious, however, whether this is the best possible choice or not. This is by no means a minor problem, since an inappropriate choice may bias the analysis and perhaps obscure chemically relevant trends. The importance of geometrical constraints in determining the actual geometry of the substituted benzene ring has been pointed out repeatedly.[11,14]

To form an unbiased, orthogonal basis for describing the geometry of monosubstituted benzene rings we have to make use of *symmetry coordinates*. These are symmetry-adapted linear combinations of the internal coordinates, transforming as the irreducible representations of the molecular point group D_{6h}.

A description of the in-plane distortion of a benzene ring in terms of nine symmetry coordinates, based on the irreducible representations of the D_{6h} point group, has been given by Murray-Rust.[28] If the distorted ring retains C_{2v} symmetry, as assumed in the present study, four of these coordinates vanish. The remaining five can be written as

$$D_1 = ({}^2/_3)^{1/2}(a + b + c) \tag{5}$$

$$D_3 = 3^{-1/2}(-a + 2b - c) \tag{6}$$

$$D_4 = 3^{-1/2}(\alpha - \beta - \gamma + \delta) \tag{7}$$

$$D_5 = 3^{-1/2}(\alpha + \beta - \gamma - \delta) \tag{8}$$

$$D_6 = 6^{-1/2}(\alpha - 2\beta + 2\gamma - \delta) \tag{9}$$

It is easily seen that D_3, D_4, D_5, and D_6 are *symmetry distortion coordinates*; i.e., they express the deviation of the ring geometry from that of unsubstituted benzene. To change D_1 into a symmetry distortion coordinate we should modify eq 5 by subtracting three times the C−C bond distance in benzene from $a + b + c$.

TABLE 2: Univariate Statistics for Internal and Symmetry Coordinates

parameter	minimum value[a]	maximum value[a]	mean[a]	variance[b]
a	1.3692	1.4482	1.3945	0.000166
b	1.3622	1.3889	1.3838	0.000016
c	1.3836	1.4030	1.3867	0.000009
α	113.13	126.37	119.04	7.07
β	116.09	123.56	120.38	2.31
γ	118.87	122.86	120.26	0.29
δ	116.07	122.81	119.69	1.01
D_1	3.3831	3.4428	3.4007	0.000104
D_3	−0.0665	0.0114	−0.0078	0.000159
D_4	−9.35	6.25	−1.11	8.90
D_5	−1.88	0.83	−0.30	0.19
D_6	−4.56	5.90	−0.37	4.20

[a] Values for *a*, *b*, *c*, D_1, and D_3 are given in Å; those for α, β, γ, δ, D_4, D_5, and D_6, in deg. [b] Values for *a*, *b*, *c*, D_1, and D_3 are given in Å^2; those for α, β, γ, δ, D_4, D_5, and D_6, in deg^2.

4. Statistics

Univariate statistics for the seven internal coordinates and five symmetry coordinates are presented in Table 2. Inspection of the table shows that, among bond angles, the largest variance occurs with α, and the smallest with γ, in agreement with the results obtained from the analysis of experimental data.[9] As regards bond distances, the variance of *a* by far outweights that of *b* and *c*, in contrast with the results of ref 9. This is not surprising, since most of the experimental bond distances used in ref 9 were from room-temperature X-ray diffraction studies, and are thus substantially affected by thermal motion effects. The librational rigid-body motions of a phenyl group that occur in the crystal cause an apparent shortening of all the ring bond distances, and particularly of the *c* distances.[9] Bond distances are also affected by nonrigid-body motions.[4] Of course, the actual extent of the shortening depends on the nature and amplitude of these motions, and varies greatly from one molecule to another. Solid-state thermal motions also affect bond angles, though to a lesser extent than bond distances.[4]

If normalized data are used, the variance of α is 5.6 times that of the *a* bond distance. This reflects the fact that stretching a C−C bond by one hundredth of its length is energetically more demanding than changing a C−C−C angle by one hundredth of its value.[29]

5. Results and Discussion

Although we have optimized at the HF/6-311++G** level the geometries of a substantial proportion of the 74 molecular species considered in the present study, we have chosen to base the discussion on the results of HF/6-31G* calculations. We have found that the two basis sets give closely similar ring geometries for most of the molecules investigated. It is only with two of the negatively charged groups (CH_2^- and SiH_2^-) that some geometrical differences emerge. In no case, however, do these differences affect the conclusions of the present study. Also the net charge transferred from the substituent into the π-system of the benzene ring (or vice versa) is only marginally affected. Using the 6-31G* basis set has proved to be a reasonable compromise between accuracy and computational effort—at least with the present class of molecules.

To present and discuss our results we make use of various scattergrams of the internal and symmetry coordinates, based on all entries of the data set. The scattergrams have been selected so as to convey important chemical information in a clear and effective way.

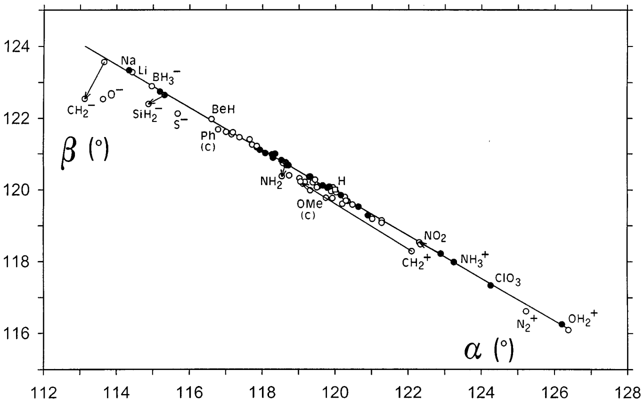

Figure 2. Scattergram of the ring angle β vs α. The correlation coefficient is $r = -0.989$ on 74 data points. The 23 nonresonant substituents used to trace the electronegativity line (see text) are marked with filled circles. The arrows connect the orthogonal and coplanar conformations of a few representative planar substituents, the arrowhead pointing toward the coplanar conformation. Also shown is the reference position of unsubstituted benzene (H).

5.1. The β vs α Scattergram. The existence of a correlation between β and α, with $\Delta\beta \simeq -\Delta\alpha/2$, was recognized quite early[5] and has a clear structural implication. It points to the fact that the angular deformation of the benzene ring occurring at the ipso position under substituent impact is largely compensated by a deformation of opposite sign at the ortho positions, with only little distortion extending further to the opposite part of the ring. This is also reflected by the variances of α, β, γ, and δ in Table 2.

A scattergram of β vs α for the present data set is shown in Figure 2. We discuss the relationship between β and α in some detail, not only in view of its structural relevance but also because of its common introduction as a constraint in the least-squares refinement of molecular models in gas-phase electron diffraction work.[19,20,30]

Inspecting the distribution of data points on the αβ plane reveals that the majority of them align almost exactly along a straight line, with the least electronegative substituents at one end, and the most electronegative at the other (*electronegativity line*). Of the relatively few outliers, none lies significantly above this line.[31] Among the outliers are all those substituents which donate more than 0.06 electrons to the π system of the benzene ring, namely CH_2^-(c), NH_2(c), NH_2(p), NHCOMe(c), O^-, OH(c), OMe(c), SiH_2^-(c), PH_2(c), S^-, and SH(c); the most prominent of these are identified in Figure 2. The deviations from the electronegativity line are generally small; they tend to increase as the π-donor character of the substituent increases. Weaker π donors, such as, e.g., BH_3^-, F, and OH_2^+(c), virtually lie on the electronegativity line.

The situation is more complex with π-acceptor substituents. Only those bearing a positive charge—namely, Be^+, CH_2^+(c), N_2^+, SiH_2^+(c), PH_3^+, and PPh_3^+—are appreciably off the electronegativity line. Surprisingly, the functional groups CH_2^+ and SiH_2^+ are displaced from the electronegativity line even when they are in the orthogonal conformation. Note that the functional groups NH_3^+, OH_2^+(c), and OH_2^+(o)—which are not π acceptors—are not displaced. This implies that the sole presence of a positive charge on the substituent is not the reason for its being off the electronegativity line.

When the conformation of a planar π-donor functional group changes from coplanar to orthogonal, the corresponding data point moves in the αβ plane, reaching (or approaching closely) the electronegativity line. With most planar π acceptors the same conformational change causes the data point to move nearly parallel to the electronegativity line. A few of such data point shifts are indicated by arrows in Figure 2, the arrowhead pointing toward the coplanar conformation.

The remaining outliers are functional groups that give rise to repulsive H···H interactions involving the ortho hydrogens, namely Ph(c) and, to a lesser extent, CMe_3(c) and CMe_3(o).

To trace the electronegativity line in Figure 2, we have chosen to use only those substituents for which the net π charge received or donated by the benzene ring (as calculated at the HF/6-31G* level, see Table 1) does not exceed 0.01 electrons. We have also excluded CH_2^+(o) and the sterically hindered substituents Ph(c), CMe_3(c), and CMe_3(o). This leaves a total of 23 data points, through which a least-squares line has been traced; the correlation coefficient is $r = -0.9996$. It is convenient to express the equation of the electronegativity line in terms of the internal distortion coordinates $\Delta\beta$ and $\Delta\alpha$:

$$\Delta\beta = -0.595(3)\Delta\alpha - 0.087(10)° \tag{10}$$

Equation 10 can be compared to the corresponding experimental equations from ref 9, namely

$$\Delta\beta = -0.591(7)\Delta\alpha - 0.301(15)° \tag{11}$$

for first-row substituents,[32] and

$$\Delta\beta = -0.615(11)\Delta\alpha - 0.384(19)° \tag{12}$$

for second-row substituents. While the difference in the angular coefficient is marginal, the intercept of eq 10 differs significantly from those of eqs 11 and 12. Note that the reference point of unsubstituted benzene, $\Delta\alpha = \Delta\beta = 0$, is closer to the present electronegativity line than to the experimental lines.

It could be argued that eqs 11 and 12 were obtained from all data points in the respective data sets, while eq 10 has been obtained from a subset of data points, excluding π-acceptor and π-donor substituents. This cannot be the sole reason for the discrepancy, however, since the regression line through all 74 data points in Figure 2 has an intercept of −0.161(29)°.

To check the effect that using a more extended basis set may have on the electronegativity line we have reoptimized at the HF/6-311++G** level 17 out of the 23 benzene ring geometries used to define that line. The regression line through these points has an angular coefficient of −0.595(4) and an intercept of −0.082(11)°, with a correlation coefficient $r = -0.9997$ − virtually the same values as in eq 10. Calculations at the MP2-(f.c.)/6-311++G** level indicate that correcting for electron correlation has only a limited effect on these figures. It is likely that most of the difference between the intercepts of the theoretical and experimental lines is due not to inadequacies in the MO calculations but rather to systematic errors in the experimental data of ref 9, such as the asphericity shifts of the atomic positions from X-ray crystallography and the effects of solid-state thermal motions.

5.2. The *a* vs α Scattergram. The rationalization of the benzene ring deformation caused by substitution in terms of hybridization effects[2−4] implies the existence of a correlation between the length of the *a* bonds and the angle α. A shift of electron density from the ipso carbon to a σ-electron-withdrawing substituent is most effectively accomplished through an increase in the p character of the sp^2 hybrid orbital of carbon pointing toward the substituent. This implies a decrease in the p character of the other two hybrid orbitals of carbon and leads, therefore, to a larger α angle and shorter *a* bonds (*electronegativity effect*). The opposite is true for a σ-electron-releasing substituent.

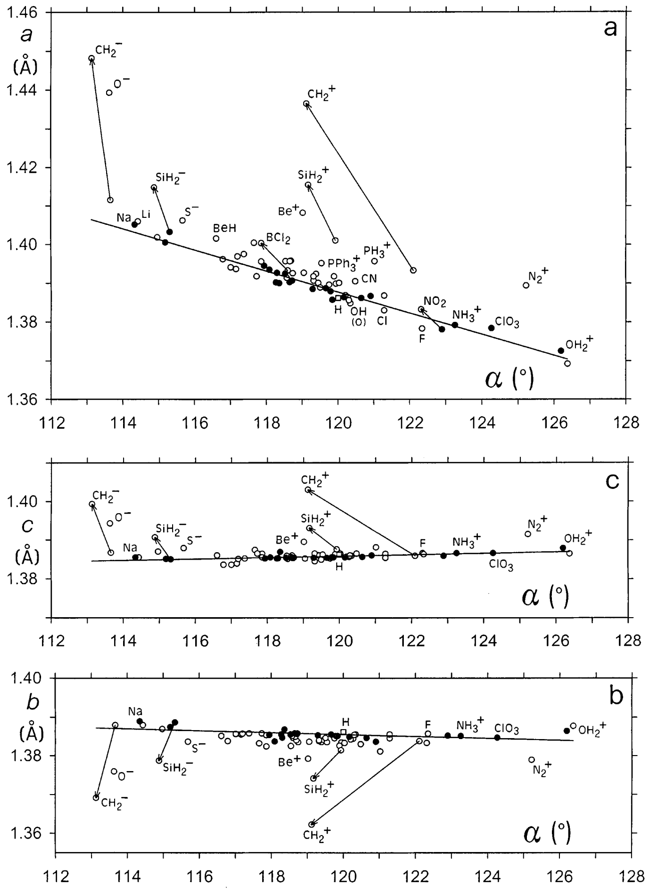

Figure 3. (a, b, c) Scattergrams of the ring C−C bond distances *a*, *b*, and *c* vs the angle α. For each scattergram an electronegativity line has been traced through 23 nonresonant substituents (see text); these are marked with filled circles. The arrows connect the orthogonal and coplanar conformations of a few representative planar substituents, the arrowhead pointing toward the coplanar conformation. Also shown is the reference position of unsubstituted benzene (H).

If the substituent has filled or unfilled orbitals of suitable size and symmetry available for mixing with the π orbitals of the benzene ring, a certain amount of π bonding may build up in the carbon-to-substituent bond, C−X. In valence bond (VB) formalism, this is described in terms of contributions from polar canonical forms to the electronic structure of the molecule. This leads to a decrease of the α angle and lengthening of the *a* bonds as the C−X bond order increases (*resonance effect*), *irrespective of whether the substituent is a π donor or a π acceptor*.[4] Again, a correlation between *a* and α is expected to exist.

A very poor correlation between *a* and α ($r = -0.56$ for 149 substituents) was reported for the experimental data of ref 9. A detailed analysis proved impossible since most of the variance of *a* was apparently due to uncorrected thermal motion effects and other inhomogeneities of the sample.

A scattergram of *a* vs α for the present data set (Figure 3a) shows that electronegativity and resonance effects are well separated in the α*a* plane. While the bulk of the data points are reasonably well aligned and exhibit the expected trend with increasing substituent electronegativity, a number of egregious outliers—all above the electronegativity line—reveal the resonance effect.

To trace the electronegativity line, we have used the same nonresonant substituents as in the β vs α scattergram. The equation of the line is best expressed in terms of internal distortion coordinates:

$$\Delta a = -0.00272(11)\Delta\alpha + 0.0015(3)\ \text{Å} \qquad (13)$$

The correlation coefficient is $r = -0.982$ on 23 data points. Equation 13 implies that an increase of α by 1° is associated with a decrease of a by 0.0027_2 Å; the same result was obtained by applying factor analysis to a set of 149 experimental geometries, see Table 6c of ref 9. HF/6-311++G** calculations on 17 out of the 23 data points yield a similar figure, 0.0028_9 Å.

For some representative planar substituents in Figure 3a the data point associated with the orthogonal conformation (where resonance is not generally expected to occur) is connected by an arrow to the corresponding data point for the coplanar conformation (where resonance is expected to be at a maximum). This displays the concerted variation of a and α caused by increasing resonance interactions, superimposed onto the electronegativity effect.

Most outliers in Figure 3a correspond to substituents that we know from Table 1 to be strong π donors or π acceptors, such as CH_2^-(c), O^-, SiH_2^-(c), S^-, BH_2(c), BCl_2(c), SiH_2^+(c), CH_2^+(c), and N_2^+. The separation of electronegativity and resonance effects originates from the fact that in the resonance effect the increase of a associated with a given decrease of α is substantially greater than the corresponding increase of a along the electronegativity line; it also varies widely from a substituent to another. The decrease of α and increase of a caused by resonance effects depend to some extent on the amount of charge accepted or donated by the π system of the benzene ring. It appears, however, that geometrical changes are generally more conspicuous with π-acceptor substituents than with π-donors.

We wish to point out that in most cases the lengthening of the a bonds due to resonance interactions is a relatively small effect. It may reach 0.03−0.04 Å with some charged substituents [CH_2^-(c), O^-, CH_2^+(c)], but is less than 0.010 Å for neutral functional groups. For instance, it is only 0.006 Å in phenylborane, 0.005 Å in aniline, and 0.004 Å in anisole. Such small changes are easily masked by other interactions involving the a bonds; see later on in this section.

A number of data points in Figure 3a deserve specific comment. Most of our comments are based on the results of natural bond orbital (NBO) analysis,[25] a technique that has proved instrumental in revealing how electron density is transferred from the benzene ring to the substituent or vice versa. All the results discussed below are confirmed by HF/6-311++G** calculations. The small changes in the geometry of the $C_{ortho}-H$ bonds are also confirmed by calculations at the MP2(f.c.)/6-311++G** level.

CH_2^-, Orthogonal Conformation. The slight displacement of this data point from the electronegativity line is due in part to hyperconjugation, some electron density (0.02 electrons) being transferred from the σ(C−H) orbitals of the substituent into the π system of the benzene ring, and in part to the interaction of the substituent lone pair with the $\sigma^*(C_{ipso}-C_{ortho})$ orbitals.

BeH, Be^+. The π-acceptor character of these substituents is due to electron density transfer from the π system of the benzene ring into an empty p orbital of the beryllium atom. The resonance effect is more pronounced in the charged species, due to the lower energy of the acceptor orbital. A further reason for the lengthening of the a bonds is probably the repulsive interaction between the ortho hydrogens and the positively charged substituent. In $C_6H_5-Be^+$ the $C_{ortho}-H$ bonds are bent by 2.0° away from the substituent and lengthened by 0.002 Å as compared to the $C_{meta}-H$ bonds. Similar distortions occur with C_6H_5-BeH. Lengthening the a bonds reduces the repulsive interaction and stabilizes the molecule.

N_2^+. The π-acceptor character of this charged substituent stems from a transfer of electron density from the π system of the benzene ring into the π^* orbital of the substituent perpendicular to the ring plane. Yet another effect contributes to the lengthening of the a bonds: it is the transfer of electron density from the $\sigma(C_{ipso}-C_{ortho})$ orbitals into the π^* orbital of the substituent in the ring plane, and from the π orbital of the substituent in the ring plane into the $\sigma^*(C_{ipso}-C_{ortho})$ orbitals.

PH_3^+ and PPh_3^+. Substituents possessing a positively charged phosphorus atom are π acceptors, due to electron density transfer from the π system of the benzene ring into the σ^*(P−H) or σ^*(P−C) and (to a lesser extent) d(P) orbitals. The effect has been termed "negative hyperconjugation".[33] It also occurs with SiH_3 and $SiPh_3$,[34] which are isoelectronic with PH_3^+ and PPh_3^+, respectively. However, the lack of a positive charge on the silicon atom makes the effect less pronounced than in phosphorus compounds. Part of the lengthening of the a bonds in $C_6H_5-PH_3^+$ and $C_6H_5-PPh_3^+$ is likely to arise from the repulsive interaction between the ortho hydrogens and the positively charged P atom, as in $C_6H_5-Be^+$ and C_6H_5-BeH.

SiH_2^+, Orthogonal Conformation. It is at first surprising that the data point corresponding to SiH_2^+(o) is so much displaced from the electronegativity line in Figure 3a. The perpendicular conformation of the substituent should prevent any transfer of electron density from the π system of the benzene ring into the empty p orbital of silicon. However, NBO analysis shows that the SiH_2^+ group acts as a π acceptor even when it assumes the orthogonal conformation, the π charge lost by the benzene ring amounting to 0.03 electrons (to be compared to 0.21 electrons in the coplanar conformation). This is due to negative hyperconjugation, as the two σ^*(Si−H) orbitals [and, to a lesser extent, a d(Si) orbital] drain electron density from the π system of the benzene ring.[35] A further reason for the lengthening of the a bonds is again the repulsive interaction between the ortho hydrogens and the positively charged Si atom. The $C_{ortho}-H$ bonds are bent by 2.6° away from the substituent, and lengthened by 0.003 Å as compared to the $C_{meta}-H$ bonds.

CH_2^+, Orthogonal Conformation. Also the data point corresponding to the orthogonal conformation of the benzyl cation is remarkably displaced from the electronegativity line in Figure 3a. Here, however, the ring-substituent interaction is more complex than in the previous case. The CH_2^+(o) group is involved in both hyperconjugation (i.e., electron density transfer from the σ(C−H) orbitals of the substituent into the π system of the benzene ring) and negative hyperconjugation (i.e., electron density transfer from the π system of the benzene ring into the σ^*(C−H) orbitals of the substituent). The two effects cooperate in making the a bonds longer.[36] But two additional effects contribute to the lengthening of the a bonds. They are as follows: (i) the transfer of electron density from the $\sigma(C_{ipso}-C_{ortho})$ bonding orbitals into the empty p orbital of the substituent in the ring plane, and (ii) the repulsive interaction between the ortho hydrogens and the positively charged substituent.

Fluorine. The position of the F data point in Figure 3a is puzzling, as it lies slightly below rather than above the electronegativity line. Fluorine is a relatively weak π donor, the transfer of electron density into the π system of the benzene ring amounting to 0.05 electrons from the present calculations. Therefore, the lengthening of the a bonds in fluorobenzene due to resonance effects should be small—a few thousandths of an angstrom—but still observable in Figure 3a. A rationale for the anomalous behavior of fluorine could be that the ortho hydrogens are strongly attracted by the fluorine atom (they are actually bent toward fluorine by 2.3°). A shortening of the *a* bonds—and, to a lesser extent, of the $C_{ortho}-H$ bonds—would favor this stabilizing interaction; indeed, the $C_{ortho}-H$ bonds in fluorobenzene are 0.001 Å shorter than the $C_{meta}-H$ bonds, at all levels of calculation. A similar effect occurs with the OH-(o) and OMe(o) groups, which also lie slightly below the electronegativity line of Figure 3a.

OH_2^+, Coplanar and Orthogonal Conformations. The OH_2^+ substituent is anomalous in that the *a* bonds are shortened by 0.003 Å, rather than lengthened, in going from the orthogonal to the coplanar conformation. The anomaly survives at all levels of calculation.

5.3. The *b* vs α and *c* vs α Scattergrams. Scattergrams of *b* and *c* vs α are reported in Figure 3, parts b and c, respectively. As in Figure 3a, the arrows connect data points associated with a few representative planar substituents in the coplanar and orthogonal conformations, the arrowhead pointing toward the coplanar conformation. Electronegativity lines have been traced through the data points associated with the same 23 nonresonant substituents as in Figures 2 and 3a. The two scattergrams show that the lengths of the *b* and *c* bonds are scarcely affected by changes in the electronegativity of the substituent but vary appreciably as the resonance interaction between the ring and the substituent increases. The variation consists of a shortening of the *b* bonds, and lengthening of the *c* bonds, by amounts that are almost invariably less than the lengthening of the *a* bonds. This is in line with an increased contribution of polar canonical forms to the electronic structure of the molecule. Note that the data point corresponding to CH_2^+(o) lies close to the electronegativity lines of Figure 3, parts b and c, at variance with Figure 3a. This supports the view that the lengthening of the *a* bonds in the orthogonal conformation of the benzyl cation is primarily due to effects other than resonance interactions (see section 5.2).

NBO analysis shows that the small lengthening of the *b* bonds occurring at both ends of the electronegativity line in Figure 3b is a stereoelectronic effect. It is due to electron density transfer from the $\sigma(C-X)$ bonding orbital into the $\sigma^*(C_{ortho}-C_{meta})$ orbitals when X is highly electropositive and from the $\sigma(C_{ortho}-C_{meta})$ bonding orbitals into the $\sigma^*(C-X)$ orbital when X is highly electronegative.

No information on the variation of *b* and *c* with the nature of the substituent could be obtained from the statistical analysis of the experimental data.[9]

5.4. The *δ* vs α and *γ* vs α Scattergrams. An early analysis of structural results from monosubstituted benzene rings, based on a limited number of accurate, low-temperature X-ray diffraction studies, showed that the internal ring angles δ and γ are affected by perturbations occurring in the π system of the benzene ring.[6] A small, but significant decrease of δ—accompanied by a similar increase of γ—was observed with several π-donor substituents; the effect disappeared when the conformation of the substituent was unfavorable to conjugation. Evidence for an increase of δ occurring with π-acceptor substituents was also given. Later on, it was shown that δ increases slightly with increasing substituent electronegativity.[9]

A scattergram of δ vs α is shown in Figure 4a. The electronegativity and resonance effects are well separated, as they give rise to differently concerted changes of the two angles. The data points of the nonresonant substituents align well along an electronegativity line, stretching from Na and Li to ClO_3 and OH_2^+(o). The equation of the line, expressed in terms of deviations from 120°, is

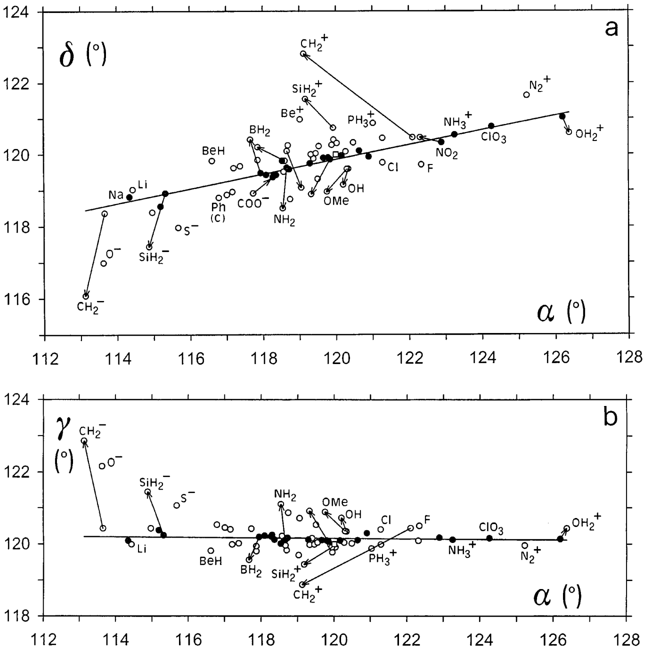

Figure 4. (a, b) Scattergrams of the ring angles δ and γ vs α. The 23 nonresonant substituents used to trace the electronegativity lines are marked with filled circles. The arrows connect the orthogonal and coplanar conformations for various planar substituents, the arrowhead pointing toward the coplanar conformation. The reference position of unsubstituted benzene is marked with an open square.

$$\Delta\delta = 0.205(9)\Delta\alpha - 0.14(3)° \qquad (14)$$

with a correlation coefficient of +0.980 on 23 data points. Equation 14 implies that increasing α by 1° causes δ to increase by 0.20_5°. HF/6-311++G** calculations on 17 out of the 23 data points yield a similar figure, 0.18_8°. These results should be compared with that obtained by applying factor analysis to 149 experimental geometries, 0.16°, from Table 6c of ref 9.

All major outliers in Figure 4a correspond to substituents that are either π-electron donors (lying below the electronegativity line) or π-electron acceptors (lying above the electronegativity line). Unlike previous scattergrams, the present one makes a clear distinction between π-donor and π-acceptor substituents. A discussion of several intriguing outliers is deferred to section 5.5.

A scattergram of γ vs α is shown in Figure 4b. This time the electronegativity line is virtually horizontal, i.e., a change in the electronegativity of the substituent has no effect on the value of γ. π-Donor and π-acceptor substituents lie on opposite sides of the electronegativity line, as in the δ vs α scattergram. We thus confirm that the ring angle γ is the best *single* angular parameter to describe resonance effects.[8]

In Figure 4, the concerted variation of δ, γ, and α caused by increasing resonance interactions is shown by arrows connecting the orthogonal and coplanar conformations of various planar substituents. The relative angular changes vary appreciably from a substituent to another, in contrast with changes associated with the electronegativity effect.

5.5. The D_4 vs D_6 Scattergram. A scattergram of the symmetry coordinates D_4 vs D_6 is shown in Figures 5 and 6. In some way it resembles the δ vs α scattergram of Figure 4a, but the resolution of the electronegativity and resonance effects is much better. This is due to the fact that D_4 and D_6 are mutually orthogonal, unlike the internal coordinates α and δ. Thus, the D_4 vs D_6 correlation does not contain contributions from the

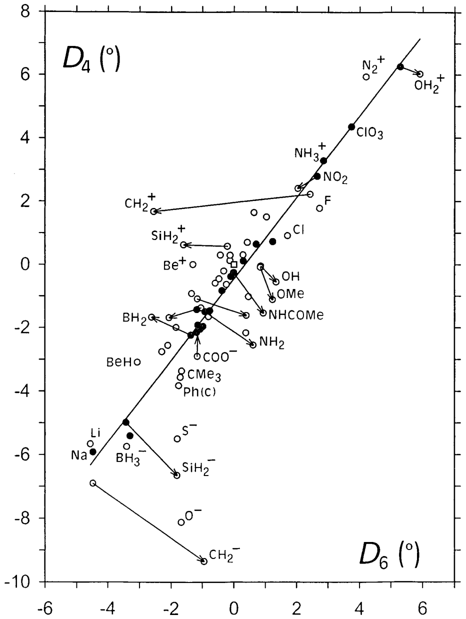

Figure 5. Scattergram of the symmetry coordinate D_4 vs D_6. The 23 nonresonant substituents used to trace the electronegativity line are marked with filled circles. The arrows connect the orthogonal and coplanar conformations for various planar substituents, the arrowhead pointing toward the coplanar conformation. The reference position of unsubstituted benzene is marked with an open square.

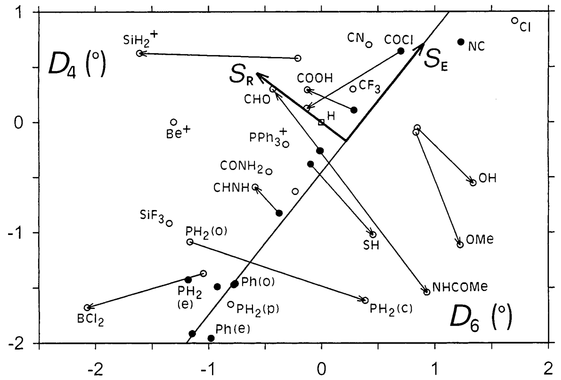

Figure 6. Enlarged view of the central area of Figure 5, showing the coordinate system used to define the structural substituent parameters S_E and S_R (see text).

purely geometrical constraint expressing the constancy of the sum of ring angles (eq 1). A contribution from this constraint is undoubtedly present in the correlation of δ with α, and even more so in the correlation of β with α.[11,13]

The electronegativity line in Figure 5 is the major axis of the D_4/D_6 distribution for the data points of the same 23 nonresonant substituents used in previous scattergrams.[37] Its equation is

$$D_4 = 1.29(3)D_6 - 0.45(6)° \qquad (15)$$

with a correlation coefficient $r = +0.996$. HF/6-311++G** calculations on 17 out of the 23 data points yield virtually the same results [$D_4 = 1.26(2)\ D_6 - 0.48(5)°$, with $r = +0.998$].

As in previous figures, the orthogonal and coplanar conformations of a planar substituent are connected by arrows, the arrowhead pointing toward the coplanar conformation. It appears that most of the arrows have their origin on, or very close to, the electronegativity line: i.e., most planar substituents show no resonance effect when they are forced to assume the orthogonal conformation. Thus, the electronegativity line makes a sharp cut between π-donor and π-acceptor substituents. The few exceptions are discussed below, together with some intriguing outliers. At variance with the results of ref 9, there appears to be no reason for separating the substituents into two groups, according to the row of the periodic table to which the first atom of the substituent belongs.

BH_3^-. The small deviation of this data point from the electronegativity line is due to hyperconjugation, i.e., electron density transfer (0.02 electrons) from the σ(B−H) bonding orbitals into the π system of the benzene ring. The same effect occurs with the orthogonal conformation of the benzyl anion, CH_2^-(o); see section 5.2.

BCl_2, Orthogonal Conformation. Negative hyperconjugation causes the BCl_2(o) group to act as a weak π acceptor: 0.01_4 electrons are transferred from the π system of the benzene ring into the σ*(B−Cl) orbitals.

CF_3 and SiF_3. These are again cases of negative hyperconjugation. The transfer of electron density from the π system of the benzene ring into the σ* orbitals of the substituents amounts to 0.02 electrons in both cases.

The Carboxylate Group. The COO^- group is the only planar substituent in our data set to act as a π donor when it assumes the orthogonal—rather than coplanar—conformation. The charge transferred to the π system of the benzene ring, 0.03 electrons, comes from the lone electron pairs of the oxygen atoms. However, the coplanar conformation corresponds to the potential energy minimum, while the orthogonal conformation is a first-order saddle point, lying 33 kJ mol^{-1} above the minimum.[38] The coplanar conformation is apparently stabilized by the strongly attractive interactions that occur between the ortho hydrogens and the negatively charged oxygen atoms. These cause the C_{ortho}−H bonds to bend by 3.5° toward the substituent and to shorten by 0.005 Å as compared to the C_{meta}−H bonds.

Biphenyl. Going from the orthogonal to the coplanar conformation of biphenyl causes the corresponding data point to shift considerably in the D_6D_4 plane; see Figures 5 and 6. The deviation from the electronegativity line is not due to resonance effects, but rather to strongly repulsive interactions between the ortho hydrogens in the coplanar conformation of the molecule (the H•••H distance in the ortho bays is only 1.97 Å from HF/6-31G* calculations,[17] much less than twice the van der Waals radius of hydrogen, 2.4 Å[39]). The effect of H•••H interactions on the internal coordinates consists of a marked decrease of the α angle (−1.9°), coupled with a lengthening of the *a* bonds (+0.006 Å), and smaller changes of the other ring angles (+1.0, +0.4, and −0.8° for β, γ, and δ, respectively).

***tert*-Butylbenzene.** H•••H repulsive interactions are also responsible for the deviation of the two data points, CMe_3(c) and CMe_3(o), from the electronegativity line of Figure 5. The deviation is slightly more pronounced in the orthogonal conformation, which is more sterically hindered than the coplanar.[20]

PH_2, Coplanar and Orthogonal Conformations. The PH_2 substituent acts as a π-electron donor when it is coplanar with the benzene ring, due to the transfer of 0.10 electrons from a 3p orbital of phosphorus into the π system of the benzene ring. It becomes a π acceptor when it assumes the orthogonal conformation, due to the transfer of 0.02 electrons from the π system of the benzene ring into the σ*(P−H) orbitals. This explains the relative positions of the two data points, PH_2(c) and PH_2(o), on opposite sides of the electronegativity line in Figure 6.

OH and OMe, Orthogonal Conformation. The deviation of these data points from the electronegativity line is due to electron density transfer from an hybrid orbital of oxygen into the π system of the benzene ring. The charge actually transferred amounts to 0.04 electrons for both OH(o) and OMe(o), as compared with 0.08 electrons for the coplanar conformations of the two molecules. That the OMe and OH groups could act as π donors also when in the orthogonal conformation was recognized quite early, from IR intensity measurements on methoxydurene[40,41] and STO-3G MO calculations of charge distribution in orthogonal phenol.[42]

OH_2^+, Coplanar Conformation, and F. The anomalous behavior of these substituents in the a vs α scattergram of Figure 3a does not seemingly affect their symmetry coordinates D_4 and D_6. The two data points are found at their expected positions in the D_4 vs D_6 scattergram.

CH_2^+, Orthogonal Conformation, and N_2^+. The anomalous position of the CH_2^+(o) data point in the D_4 vs D_6 scattergram is likely to arise from the remarkable lengthening of the a bonds occurring in this species (see section 5.2). Lengthening the a bonds (without changing α) implies a decrease of β and an increase of γ, causing the D_6 symmetry coordinate to become more positive without any change in D_4. A similar effect apparently occurs with N_2^+, making the corresponding data point closer to the electronegativity line than one would expect from the π charge actually lost by the benzene ring, 0.12 electrons.

5.6. Structural Substituent Parameters. The good separation of electronegativity and resonance effects in the D_4 vs D_6 scattergram suggests a straightforward procedure for quantifying these effects. Let the D_6D_4 reference system be changed into an S_ES_R reference system (Figure 6), whereby S_E lies on the electronegativity line, S_R is orthogonal to S_E, and the origin is set at the point where unsubstituted benzene ($D_4 = D_6 = 0$) projects onto the electronegativity line ($D_4 = -0.17°$, $D_6 = 0.22°$). It is natural to use S_E and S_R values to measure the electronegativity and resonance effects of a substituent, respectively, as seen from their impact on the benzene ring geometry. The term *structural substituent parameters* appears to be appropriate for these quantities. S_E and S_R values are calculated from the following equations:

$$\begin{aligned} S_E &= 0.790D_4 + 0.613D_6 \\ &= 0.706\Delta\alpha - 0.956\Delta\beta + 0.044\Delta\gamma + 0.206\Delta\delta \end{aligned} \tag{16}$$

$$\begin{aligned} S_R &= 0.613D_4 - 0.790D_6 + 0.28° \\ &= 0.031\Delta\alpha + 0.291\Delta\beta - 0.999\Delta\gamma + 0.677\Delta\delta + 0.28° \end{aligned} \tag{17}$$

Equations 16 and 17 are strikingly similar to the corresponding equations from the experimental study (eqs 43 and 44 of ref 9), notwithstanding the different nature of the two data sets and the different procedure used to separate electronegativity and resonance effects.[43]

In the above treatment the coordinate S_R is orthogonal to S_E. This fits the idea that electronegativity and resonance effects, as determined from reactivity data, are mutually independent and can thus be represented on orthogonal axes.[44] However, it appears from Figures 5 and 6 that the arrows connecting the orthogonal and coplanar conformations of planar functional groups are seldom orthogonal to the electronegativity axis; rather, they tend to be more or less bent toward lower electronegativities. This is by no means surprising. It is expected that both the electronegativity and resonance effects of a planar group X change continuously with the twist angle, since as the C−X bond becomes shorter due to increasing double-bond character the shape and size of the σ(C−X) bonding orbital also change.[9] The accumulation of electron density along the C−X bond as it becomes shorter makes X less electronegative.

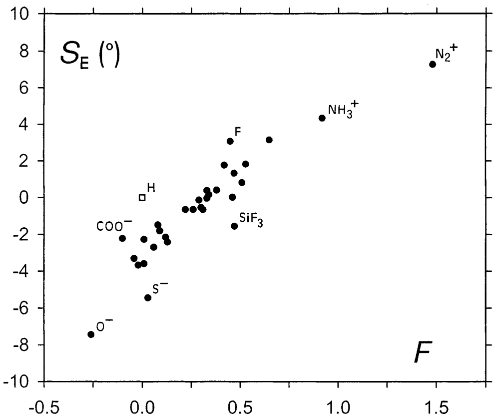

Figure 7. Plot of the structural substituent parameter S_E vs the inductive parameter F (values from Table 1 of ref 45). The correlation coefficient is +0.922 on 31 data points.

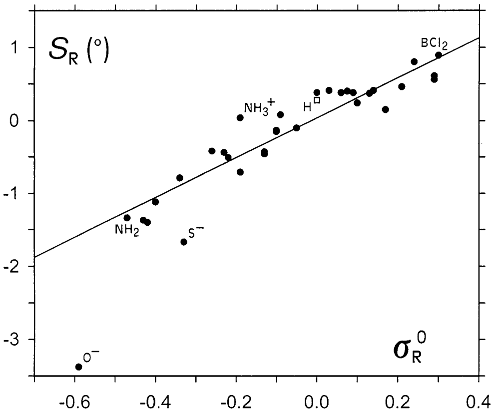

Figure 8. Plot of the structural substituent parameter S_R vs the resonance parameter σ_R^0, as obtained from infrared intensities (values from Tables 5 and 6 of ref 41 and from ref 46). The correlation coefficient is +0.907 on 33 data points; it increases to +0.959 when the charged substituents O^-, S^-, and NH_3^+ are not included.

Structural substituent parameters for all substituents in our data set are reported in Table 1. The S_E values correlate reasonably well with traditional inductive parameters from reactivity data, such as σ_I[44] or F;[45] see Figure 7. S_R values are best compared to σ_R^0 parameters from infrared intensities,[41] since these, like S_R, are derived from a physical property of the monosubstituted benzene ring. The correlation of S_R with σ_R^0 is indeed reasonable, see Figure 8, and improves substantially when some of the charged substituents are excluded. It should of course be considered that S_E and S_R values from MO calculations measure the effect of a substituent on the carbon skeleton of the benzene ring in a particular conformation of a motionless, isolated molecule, while σ_I (or F) and σ_R^0 measure the substituent effect for a real, vibrating molecule in the solution state. The electronic effects of charged substituents may be considerably altered by interactions with counterions and polar solvent molecules, particularly in hydrogen-bonded solvents.

Although π-donor and π-acceptor substituents lie on opposite sides of the electronegativity axis of Figures 5 and 6 and thus have S_R values of opposite sign, there is no doubt that the amount of charge accepted or donated by the π system of the benzene ring is not the only factor determining the value of S_R. Other factors, which are currently being investigated, are also of importance.

The use of structural substituent parameters from MO calculations as a measure of electronic substituent effects in benzene derivatives has some definite advantages over the use of other, traditional measurements of substituent effects. (1) Structural substituent parameters are obtained directly from the geometries of monosubstituted benzene rings, with no need of introducing a second substituent to act as a probe, as is generally the case in reactivity studies. The presence of the second substituent may influence the interaction of the first substituent with the ring. (2) They do not originate from a specific site of the benzene ring; instead, they express the overall angular distortion of the carbon skeleton under substituent impact. (3) They refer to the isolated molecule and so are free of interference from solvent effects. These can of course be modeled by introducing solvent molecules at appropriate positions in the MO optimization. (4) They are easily calculated for different conformations of the same molecule, including conformations (and molecules) not easily amenable to experimental structural studies.

We realize, of course, that the actual values of S_E and S_R from MO calculations may depend on the level of calculation. On the other hand, experimental geometries of adequate accuracy to derive reliable structural substituent parameters are presently only available for a limited number of free molecules. This points to the need of further, more accurate experimental and computational studies of the structure of monosubstituted benzene derivatives.

6. Conclusions

The present analysis shows that the geometry of the carbon skeleton of a monosubstituted benzene ring, as determined from MO calculations, contains valuable information on the electronegativity, resonance, and steric effects of the substituent, and also on other, more subtle effects. The results obtained are outlined below; they improve, revise, and substantially augment previous knowledge from the analysis of experimental geometries.[9]

(1) Going from a less electronegative to a more electronegative substituent causes a remarkable increase of the ring angle at the ipso position, α. The range of values is 113−126°. As α increases by 1°, the following changes occur concertedly in the geometry of the carbon hexagon: $\Delta\beta = -0.595°$, $\Delta\delta = +0.205°$, $\Delta a = -0.00272$ Å. No appreciable change occurs in the internal coordinates γ, b, and c.

(2) An excellent linear correlation exists between the ring angles β and α (the correlation coefficient is $r = -0.989$ on 74 data points). Among the relatively few outliers are the strong (and moderately strong) π-electron donors, the charged π-electron acceptors, and the sterically hindered substituents.

(3) Enhancing the resonance interaction between a substituent and the benzene ring causes a complex pattern of angular distortions, arising from the superposition of two separate effects. The first originates from the decreased length of the C−X bond. It consists primarily in a decrease of α and increase of β, and occurs irrespective of whether the substituent is a π donor or a π acceptor. The second effect is associated with π-charge alternation on the ring carbons. It involves all the internal ring angles, and depends on the substituent being a π donor or a π acceptor. π-Donor substituents cause a decrease of β and δ and an increase of α and γ; the reverse is true for π-acceptor substituents. As the two effects are superimposed, the variation of α and β is exalted with π-acceptor substituents and depressed with π-donor substituents. The angular changes are generally accompanied by lengthening of the c and especially of the a bonds, and shortening of the b bonds, as expected from an enhanced contribution of polar canonical forms to the electronic structure of the molecule.

(4) A number of planar substituents are capable of interacting with the π-electron system of the benzene ring also when they assume the orthogonal conformation. Some of them act as π donors, either by way of hyperconjugation or by using appropriately oriented lone electron pairs. Others act as π acceptors, due to negative hyperconjugation. These effects also occur with tetrahedral substituents.

(5) The electronegativity and resonance effects of a substituent are best separated in a scattergram of the symmetry coordinates D_4 and D_6. The data points of those substituent which are not sterically hindered and are neither π donors nor π acceptors align nicely along an electronegativity axis. The resonant substituents are scattered on each side of that axis, according to their being π acceptors or π donors. This makes it possible to associate to each substituent two orthogonal *structural substituent parameters*, S_E and S_R, measuring its electronegativity and resonance effects, respectively, as seen from their impact on the benzene ring geometry. S_E and S_R values for common functional groups correlate reasonably well with traditional measurements of inductive and resonance effects, respectively. They have the advantage of having been derived from a physical property of the monosubstituted benzene ring—namely, its angular distortion under substituent impact—and of being free of interference from solvent effects.

(6) Steric hindrance resulting from short contacts between the ortho hydrogens and some of the hydrogen atoms of the substituent gives rise to a marked decrease of S_E, coupled with a lesser decrease of S_R, causing the data point to shift below the electronegativity line in the D_6D_4 plane. Associated with these changes is an appreciable lengthening of the a bonds.

(7) There is evidence that the length of the a bonds is affected not only by the electronegativity, resonance, and steric effects of the substituent but also by other, more subtle effects. These include (i) electron density transfer from the $\sigma(C_{ipso}-C_{ortho})$ bonding orbitals into an empty orbital of the substituent lying in the plane of the benzene ring, (ii) electron density transfer from a filled orbital of the substituent lying in the ring plane into the $\sigma^*(C_{ipso}-C_{ortho})$ orbitals, and (iii) electrostatic interactions between the ortho hydrogens and the substituent. The role of these effects in determining the length of the a bonds cannot generally be ignored.

(8) Subtle stereoelectronic effects influence the length of the b bonds; they are only appreciable with the most electropositive or electronegative substituents.

References and Notes

(1) Keidel, F. A.; Bauer, S. H. *J. Chem. Phys.* **1956**, *25*, 1218. A recent reinvestigation[30] confirms the results of this early study.

(2) Carter, O. L.; McPhail, A. T.; Sim, G. A. *J. Chem. Soc. A* **1966**, 822.

(3) Nygaard, L.; Bojesen, I.; Pedersen, T.; Rastrup-Andersen, J. *J. Mol. Struct.* **1968**, *2*, 209.

(4) Domenicano, A.; Vaciago, A.; Coulson, C. A. *Acta Crystallogr., Sect. B* **1975**, *31*, 221.

(5) Domenicano, A.; Vaciago, A.; Coulson, C. A. *Acta Crystallogr., Sect. B* **1975**, *31*, 1630.

(6) Domenicano, A.; Vaciago, A. *Acta Crystallogr., Sect. B* **1979**, *35*, 1382.

(7) Domenicano, A.; Mazzeo, P.; Vaciago, A. *Tetrahedron Lett.* **1976**, 1029.

(8) Domenicano, A.; Murray-Rust, P. *Tetrahedron Lett.* **1979**, 2283.

(9) Domenicano, A.; Murray-Rust, P.; Vaciago, A. *Acta Crystallogr., Sect. B* **1983**, *39*, 457.

(10) Campos, J. A.; Casado, J.; Ríos, M. A. *J. Am. Chem. Soc.* **1980**, *102*, 1501.

(11) Ríos, M. A.; Vázquez, L. *An. Quím., Ser. A* **1986**, *82*, 170.

(12) Vázquez, L.; Ríos, M. A. *Mol. Phys.* **1988**, *65*, 129.

(13) Vázquez, L.; Estévez, C. M.; Ríos, M. A. *J. Chim. Phys.* **1990**, *87*, 565.

(14) Vázquez, L.; Ríos, M. A. *J. Phys. Chem.* **1992**, *96*, 6624.

(15) Von Nagy-Felsobuki, E.; Topsom, R. D.; Pollack, S.; Taft, R. W. *J. Mol. Struct. (THEOCHEM)* **1982**, *88*, 255. Bock, C. W.; Trachtman, M.; George, P. *J. Mol. Struct. (THEOCHEM)* **1985**, *122*, 155. Krygowski, T. M.; Häfelinger, G.; Schüle, J. *Z. Naturforsch., Teil B* **1986**, *41*, 895. Exner, O.; Böhm, S. *Acta Crystallogr., Sect. B* **2002**, *58*, 877.

(16) Campanelli, A. R.; Domenicano, A.; Ramondo, F. Work in progress.

(17) Tsuzuki, S.; Tanabe, K. *J. Phys. Chem.* **1991**, *95*, 139.

(18) Colapietro, M.; Domenicano, A. *Acta Crystallogr., Sect. B* **1978**, *34*, 3277. Konschin, H. *J. Mol. Struct. (THEOCHEM)* **1983**, *105*, 213. Bock, C. W.; Trachtman, M.; George, P. *Chem. Phys.* **1985**, *93*, 431. Portalone, G.; Schultz, G.; Domenicano, A.; Hargittai, I. *Chem. Phys. Lett.* **1992**, *197*, 482 and references therein. Krygowski, T. M.; Anulewicz, R.; Hiberty, P. C. *J. Org. Chem.* **1996**, *61*, 8533. Krygowski, T. M.; Wisiorowski, M.; Howard, S. T.; Stolarczyk, L. Z. *Tetrahedron* **1997**, *53*, 13027 and references therein.

(19) Schultz, G.; Portalone, G.; Ramondo, F.; Domenicano, A.; Hargittai, I. *Struct. Chem.* **1996**, *7*, 59.

(20) Campanelli, A. R.; Ramondo, F.; Domenicano, A.; Hargittai, I. *J. Phys. Chem.* **1994**, *98*, 11046.

(21) Poirier, R.; Kari, R.; Csizmadia, I. G. *Handbook of Gaussian Basis Sets: A Compendium for ab Initio Molecular Orbital Calculations*; Elsevier: Amsterdam, 1985.

(22) Pulay, P. *Mol. Phys.* **1969**, *17*, 197.

(23) Frisch, M. J.; Trucks, G. W.; Schlegel, H. B.; Scuseria, G. E.; Robb, M. A.; Cheeseman, J. R.; Zakrzewski, V. G.; Montgomery, J. A., Jr.; Stratmann, R. E.; Burant, J. C.; Dapprich, S.; Millam, J. M.; Daniels, A. D.; Kudin, K. N.; Strain, M. C.; Farkas, O.; Tomasi, J.; Barone, V.; Cossi, M.; Cammi, R.; Mennucci, B.; Pomelli, C.; Adamo, C.; Clifford, S.; Ochterski, J.; Petersson, G. A.; Ayala, P. Y.; Cui, Q.; Morokuma, K.; Malick, D. K.; Rabuck, A. D.; Raghavachari, K.; Foresman, J. B.; Cioslowski, J.; Ortiz, J. V.; Stefanov, B. B.; Liu, G.; Liashenko, A.; Piskorz, P.; Komaromi, I.; Gomperts, R.; Martin, R. L.; Fox, D. J.; Keith, T.; Al-Laham, M. A.; Peng, C. Y.; Nanayakkara, A.; Gonzalez, C.; Challacombe, M.; Gill, P. M. W.; Johnson, B.; Chen, W.; Wong, M. W.; Andres, J. L.; Gonzalez, C.; Head-Gordon, M.; Replogle, E. S.; Pople, J. A. *Gaussian 98, Revision A.6*; Gaussian Inc.: Pittsburgh, PA, 1998.

(24) Møller, C.; Plesset, M. S. *Phys. Rev.* **1934**, *46*, 618.

(25) Reed, A. E.; Weinhold, F. *J. Chem. Phys.* **1985**, *83*, 1736. Reed, A. E.; Curtiss, L. A.; Weinhold, F. *Chem. Rev.* **1988**, *88*, 899.

(26) Glendening, E. D.; Reed, A. E.; Carpenter, J. E.; Weinhold, F. *NBO 3.0 Program*; University of Wisconsin: Madison, WI.

(27) Britton, D. *Acta Crystallogr., Sect. B* **1977**, *33*, 3727.

(28) Murray-Rust, P. *Acta Crystallogr., Sect. B* **1982**, *38*, 2818.

(29) Bernstein, J. In *Accurate Molecular Structures: Their Determination and Importance*; Domenicano, A., Hargittai, I., Eds.; Oxford University Press: Oxford, 1992; Chapter 19. Hargittai, I.; Levy, J. B. *Struct. Chem.* **1999**, *10*, 387.

(30) Portalone, G.; Ramondo, F.; Domenicano, A.; Hargittai, I. *J. Organomet. Chem.* **1998**, *560*, 183.

(31) The experimental study[9] gave no evidence for outliers in the β vs α scattergram.

(32) Here we retain the original terminology used in refs 4, 5, and 9, whereby a substituent is termed first-row (second-row) when it is bonded to the benzene ring through an atom of the Li-to-F (Na-to-Cl) row of the periodic table.

(33) Schleyer, P. v. R.; Kos, A. J. *Tetrahedron* **1983**, *39*, 1141.

(34) Campanelli, A. R.; Ramondo, F.; Domenicano, A.; Hargittai, I. *J. Phys. Chem. A* **2001**, *105*, 5933.

(35) The effect of negative hyperconjugation is also seen in the length of the two Si−H bonds, which increases by 0.003 Å in going from the coplanar to the orthogonal conformation.

(36) The two effects also cooperate in lengthening the C−H bonds of the substituent, as r(C−H) increases by 0.007 Å in going from the coplanar to the orthogonal conformation of the benzyl cation.

(37) It would be inappropriate to use regression here as we cannot regard one variable as dependent on the other.

(38) The corresponding figure from HF/6-311++G** calculations is 25 kJ mol^{-1}.

(39) Pauling, L. *The Nature of the Chemical Bond*, 3rd ed.; Cornell University Press: Ithaca, NY, 1960; p 260.

(40) Brownlee, R. T. C.; Hutchinson, R. E. J.; Katritzky, A. R.; Tidwell, T. T.; Topsom, R. D. *J. Am. Chem. Soc.* **1968**, *90*, 1757.

(41) Katritzky, A. R.; Topsom, R. D. *Chem. Rev.* **1977**, *77*, 639.

(42) Hehre, W. J.; Radom, L.; Pople, J. A. *J. Am. Chem. Soc.* **1972**, *94*, 1496.

(43) Due to the linear relationship between $\Delta\beta$ and $\Delta\alpha$ (eq 10 for nonresonant substituents) and the relatively small coefficients of $\Delta\gamma$ and $\Delta\delta$ in eq 16, α values can be used directly as an approximate measure of electronegativity effects,[5] except for strong π-donor and π-acceptor substituents.

(44) Ehrenson, S.; Brownlee, R. T. C.; Taft, R. W. *Prog. Phys. Org. Chem.* **1973**, *10*, 1 and references therein.

(45) Hansch, C.; Leo, A.; Taft, R. W. *Chem. Rev.* **1991**, *91*, 165.

(46) Angelelli, J. M.; Brownlee, R. T. C.; Katritzky, A. R.; Topsom, R. D.; Yakhontov, L. *J. Am. Chem. Soc.* **1969**, *91*, 4500.